Ataxia-Telangiectasia Mutated (ATM) Protein Signaling Participates in Development of Pulmonary Arterial Hypertension in Rats

Authors' Contribution:
Study Design A
Data Collection B
Statistical Analysis C
Data Interpretation D
Manuscript Preparation E
Literature Search F
Funds Collection G

BCEF 1,2 Fan Hu*
BCDF 1,2 Caijun Liu*
AEG 1,2 Hanmin Liu
AD 1,2 Liang Xie
D 1,2 Li Yu

1 Department of Pediatrics, West China Second University Hospital of Sichuan University, Chengdu, Sichuan, P.R. China
2 Key Laboratory of Birth Defects and Related Diseases of Women and Children, Sichuan University, Ministry of Education, Chengdu, Sichuan, P.R. China

Corresponding Author:
Source of support:

* Co-first author; Fan Hu and Caijun Liu contributed equally to this study. They are co-first authors
Hanmin Liu, e-mail: hanmin@vip.163.com
This work was supported by the National Natural Science Fund of China (grant number 81370220)

Background: Previous studies revealed physiological and pathogenetic similarity between vascular smooth muscles cells with severe pulmonary arterial hypertension and tumors. The DNA damage response was found in both pulmonary arterial hypertension (PAH) cells and tumors. The ataxia-telangiectasia mutated proteins (ATM) pathway is considered an important factor in the DNA damage response of tumor formation, but its function in the development of PAH remains unknown.

Material/Methods: The Sprague-Dawley rat PAH model was established. Three weeks (Group M1), 5 weeks (Group M2), and 7 weeks (Group M3) after drug injection, pulmonary expression of ATM, Checkpoint kinase 2 (Chk2), P53, and P21 were measured. A section of the lungs from Group M2 was used for pulmonary artery vascular smooth muscles cells (PA-SMCs) isolation and culture. The effect of KU60019 in the proliferation and apoptosis of primary cultured rat PA-SMCs was measured by 3-(4,5-dimethyl-2-thiazolyl)-2,5-diphenyl-2-H-tetrazolium bromide (MTT) and TdT-mediated dUTP nick-end labeling (TUNEL), respectively.

Results: Immunohistochemistry results show that the expression of ATM, Chk2, and P21 increased in Groups M1 and M2, and decreased in Group M3. Additionally, expression of P53 increased in Group M1, and decreased in Groups M2 and M3. RT-PCR and Western blotting demonstrated that in Groups M1 and M2, the expression of ATM, Chk2, P53, and P21 increased, whereas it decreased in Group M3. In cell culture, 0.3 µM and 0.5 µM KU60019 increased the growth of PA-SMCs, and 0.5 µM KU60019 reduced cell apoptosis.

Conclusions: Expression of the ATM-Chk2 pathway increased in early stages of PAH formation, but decreased in late stages. In primary cultured PA-SMCs, KU60019 increased cell proliferation and inhibited cell apoptosis.

MeSH Keywords: Apoptosis • Ataxia Telangiectasia Mutated Proteins • Cell Proliferation • Pulmonary Artery

Full-text PDF: https://www.medscimonit.com/abstract/index/idArt/906568

📄 2680   ▦ 2   📊 4   📑 29

Background

Pulmonary arterial hypertension (PAH), characterized by chronically increased pulmonary vascular resistance and poor prognosis, is a common cardiovascular disease [1]. Pulmonary vascular remodeling is the primary pathological change [2–4]. Intimal thickening and plexiform lesions are observed in both primary pulmonary hypertension and Eisenmenger's syndrome. Most intimal cells with intimal lesions showed an immunoprofile of myofibroblasts that were positive for vimentin and alpha-smooth muscle actin [2]. The pulmonary artery vascular smooth muscles cells (PA-SMCs) are considered as important factors in vascular activity, vascular modeling, and the maintenance of vascular tension [5,6]. Congenital heart diseases (CHDs), such as ventricular septal defects and patent ductus arteriosus, are the most important factors inducing PAH in childhood. In the early stages of PAH induced by CHDs, when there is no pulmonary vascular remodeling, the proliferation of PA-SMCs stops and is reversible if the CHD is cured. At an advanced stage, when obstructive pulmonary hypertension is formed, the proliferation of PA-SMCs is uncontrollable and irreversible. The inflection point and the key regulation factor in the progress of PAH that changes reversible PA-SMC proliferation to irreversible damage remain unknown; it is also unknown when the inflection point emerges and how the key regulation factor functions.

A previous study found a similarity between tumors and the vascular lesions in severe PAH in the following aspects: angiogenesis, evasion of apoptosis, self-sufficiency in growth signals, insensitivity to anti-growth signals, tissue invasion and metastasis, and limitless replicative potential [7]. Cancer-like pathways were found in the pathomechanisms of vascular lesions in severe pulmonary hypertension; furthermore, the use of drugs targeted at neoplasms has been suggested for the treatment of severe PAH [8].

To maintain genome stability after DNA damage, there exists a series of regulation mechanisms to detect and rapidly repair DNA damage [9,10]. The molecular network for maintaining genetic stability is called the DNA damage response (DDR). Many studies based on tumors revealed that the ataxia-telangiectasia mutated (ATM) gene, whose malfunction participates in the pathogenesis of tumors, is the core regulator factor of the DDR network [11,12]. Previous studies suggested that the inhibition of ATM or its downstream genes could increase the risk of cancer [13,14]. However, DDR was also found in pulmonary vascular remodeling [15,16]. A study of PAH patients revealed the existence of a DNA mutation in endothelium cells and PA-SMCs [15]. The function of the ATM gene in DDR is clear for the formation of tumors; however, whether it also exerts an effect on pulmonary vascular remodeling, where DDR is also present, remains unknown. Based on the

aforementioned studies, we hypothesized that the ATM pathway participates in the proliferation or apoptosis of PA-SMCs.

In this study, we measured expression changes in the ATM-Chk2 pathway in a rat PAH model induced by left lung recession plus a monocrotaline (MCT) injection. Moreover, we examined the effect of KU60019, an ATM inhibitor, on the proliferation and apoptosis of primary cultured PA-SMCs.

Animal model and methods

Animal model

All Sprague-Dawley rats (SD rats) were purchased from Chengdu Dashuo Biological Technology Co Ltd. The Experiment Animal Administrative Committee of Sichuan University approved all animal procedures for this study.

Group M (PAH model)

Male SD rats (350–400 g) underwent left lung resection and were injected subcutaneously with MCT (60 mg/kg) 1 week after surgery. Three weeks (Group M1), 5 weeks (Group M2), and 7 weeks (Group M3) after drug injection, the pulmonary expression of ATM, Chk2, P53, and P21 was measured in each rat.

Group C (control Group)

The pulmonary expression of ATM, Chk2, P53, and P21 was measured in 8 male SD rats (350–400 g) with no treatment.

Material and Methods

Pressure and stereology analysis

Rats were anesthetized by chloral hydrate. Before euthanasia, the mean pulmonary artery pressure (PAP) was measured by a transvenous catheter through the jugular vein. After the rats were sacrificed, the heart was dissected to measure the weight of the right ventricle (RV), and the weight of the left ventricle and ventricular septum (LV+S); these values were used to calculate RV/(LV+S) and evaluate the hypertrophy of RV. One part of the right lung tissue was embedded in paraffin for hematoxylin and eosin (HE) staining and immunohistochemistry studies; the other part was used for RT-PCR and Western blot assays.

Immunohistochemistry

Immunohistochemistry was used to evaluate the expression of ATM pathway genes on PA-SMCs. We chose representative genes: ATM/phosphorylated ATM, Chk2, P53/phosphorylated

Table 1. Primary and secondary antibodies used for immunohistochemistry.

Antibody	Host	Dilution	Company
ATM (primary)	Mouse	1: 200	Abcam (ab78)
Phosphorylated ATM (primary)	Mouse	1: 200	Abcam (ab36810)
Chk2 (primary)	Rabbit	1: 100	Abcam (ab47433)
P53 (primary)	Mouse	1: 400	Abcam (ab26)
Phosphorylated P53 (primary)	Rabbit	1: 100	Abcam (ab33889)
P21 (primary)	Rabbit	1: 300	Abcam (ab109199)
Envision™ Detection Kit (secondary)			Dako (K5007)

Table 2. Primary antibodies used for Western blot.

Antibody	Host	Dilution	Company
ATM	Mouse	1: 1000	Abcam (ab78)
Chk2	Rabbit	1: 1000	Abcam (ab47433)
P53	Mouse	1: 2000	Abcam (ab26)
P21	Rabbit	1: 1000	Abcam (ab109199)

P53, and P21. Immunohistochemistry techniques were performed as follow. First, sliced samples were dehydrated in the following steps: 3 times in dimethylbenzene for 5 min each, twice in 100% ethanol for 3 min each, in 90% and 70% ethanol for 3 min each, washed with water for 3 min, in double-distilled water for 3 min, and washed 3 times in phosphate-buffered saline (PBS) for 3 min. After dehydration, the EDTA antigen retrieval solution (pH 9.0) was added to the samples for antigen retrieval in a 97°C water bath for 40 min. After natural cooling, the samples were washed 3 times with PBS for 3 min each. Then, the samples were incubated with 3% H_2O_2 for 15 min and washed again 3 times with PBS for 3 min each. The samples were incubated with primary antibody (Table 1) at 37°C for 45 min and washed 3 times with PBS for 3 min each. Next, the samples were incubated with secondary antibody (Table 1) at 37°C for 45 min and washed 3 times with PBS for 3 min. Then, the diaminobenzidine (DAB; 100 μL) chromogenic reagent was added to the samples. After coloration, samples were washed with distilled water.

Real-time polymerase chain reaction (RT-PCR)

RT-PCR of the right lung was used to detect the expression of ATM, Chk2, P53, and P21. The primer sequences were as follows:
ATM: forward: 3'-GCTTATGACGTTGCATGAAACG-5'
reverse: 3'-GTGACGGGAAATATGGTGGATT-5'
Chk2: forward: 3'-AAGAGACGAATACATCATGTCAAAAACT-5'
reverse: 3'-GGCCACTTTCTTACACGTTTTCC-5'
P53: forward: 3'-TCCTCCCCAACATCTTATCC-5'

reverse: 3'-GCACAAACACGAACCTCAAA-5'
P21: forward: 3'-CGGGCAGTCCCTTCTAGTTCC-5'
reverse: 3'-AATGCTTGAGCACACACGAG-5'

The conditions for the RT-PCR amplification were as follows: ATM and glyceraldehyde 3-phosphate dehydrogenase (GAPDH): 95°C for 10 s, 60°C for 30 s, and 72°C for 30 s (40 cycles).
Chk2 and GAPDH: 95°C for 10 s, 58°C for 30 s, and 72°C for 30 s (40 cycles).
P53 and GAPDH: 95°C for 10 s, 58°C for 30 s, and 72°C for 30 s (40 cycles).
P21 and GAPDH: 95°C for 10 s, 58°C for 30 s, and 72°C for 30 s (40 cycles).

Western blotting

Lung tissue stored at –80°C was used for Western blotting. The samples were lysed in a buffer with phosphatases and protease inhibitors. The proteins (200 μg) were loaded in a 4–12% Bis-Tris gel (Life Technologies, Carlsbad, USA) and transferred onto PVDF membranes (Merck Millipore, Germany). The membranes were incubated with the antibodies described in Table 2 overnight at 4°C. Antibody binding was detected by an anti-mouse HRP secondary antibody (ab97040, Abcam, UK) and visualized with the ECL development solution (ab133406, Abcam, UK). The Gel-Pro analyzer was used to measure the integrated optical density (IOD) of the samples.
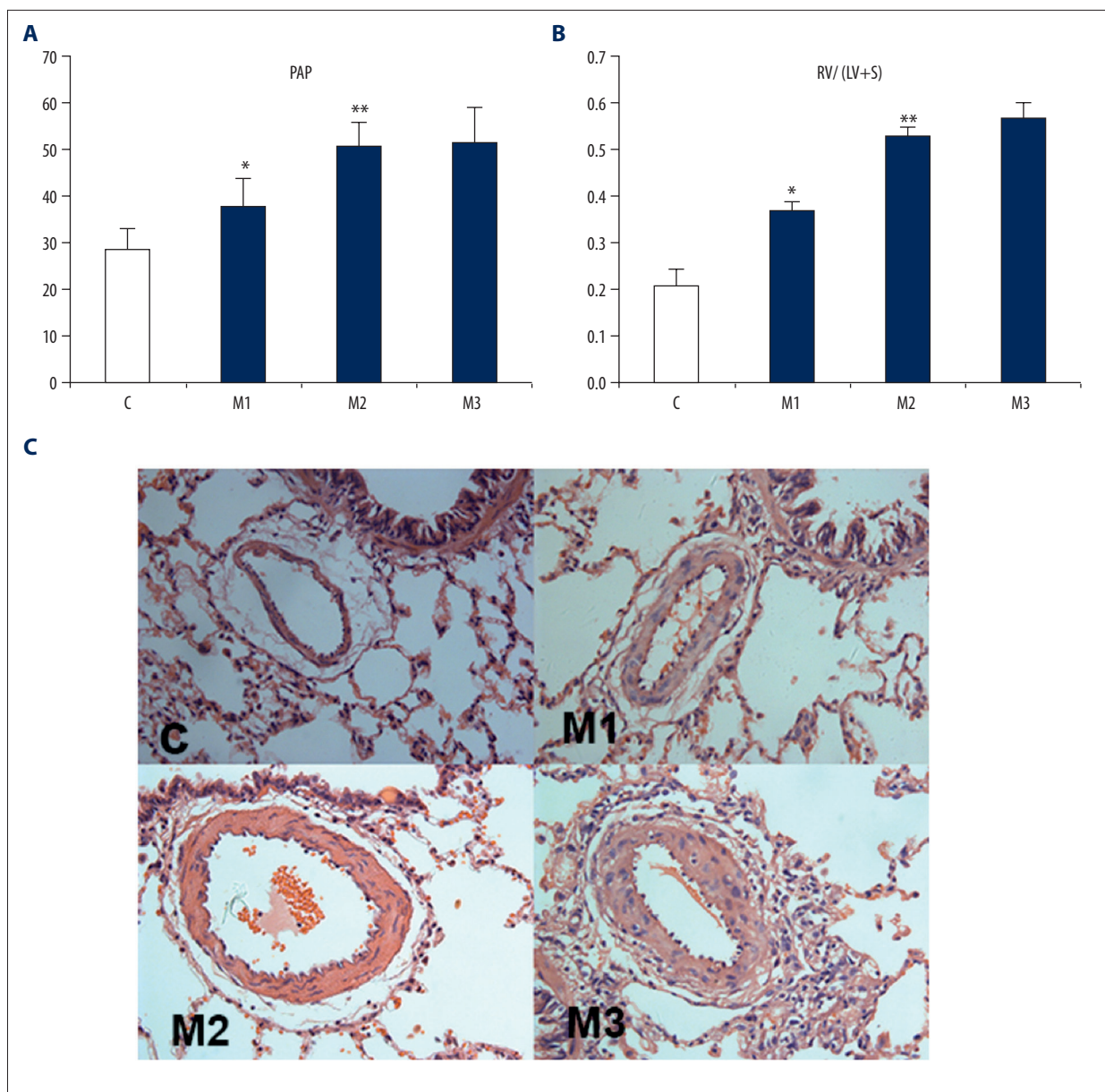
Figure 1. (**A**) * The PAP was higher in Group M1 compared with Control Group (Group C) (p=0.02). ** The pressure was significantly higher in Group M2 compared with Group C (p<0.01) and Group M1 (p<0.01). (**B**) RV/(LV+S) continued to increase in Group M1 and Group M2 compared with the Control Group (Group C) (p<0.05). * p<0.01 *vs.* Group C, ** p<0.01 *vs.* Group C, p=0.02 *vs.* Group M1. (**C**) HE staining of right lungs in Control Group (A), Group M1 (B), Group M2 (C), and Group M3 (D). The figure demonstrates a normal arteriole in the Control Group and severe vascular lesions in Group M2 and Group M3, suggesting the formation of severe PAH (×400).

Primary PA-SMCs isolation and culture

A few parts of the lungs from Group M2, in which ATM expression was increased, were used for PA-SMCs isolation and culture. Rat PA-SMCs were isolated and cultured following the protocol previously described by Yin [17]. Assays were performed at passages 3-5. The 3-(4,5-dimethyl-2-thiazolyl)-2,5-diphenyl-2-H-tetrazolium bromide (MTT) assay was used to

evaluate cell proliferation and the TdT-mediated dUTP nick-end labeling (TUNEL) assay was used to measure apoptosis.

Proliferation of PA-SMACs

The MTT assay was used to assess the proliferation of PA-SMACs treated with different concentrations of KU60019 (Selleck, Houston, USA), an ATM inhibitor. Cells were cultured
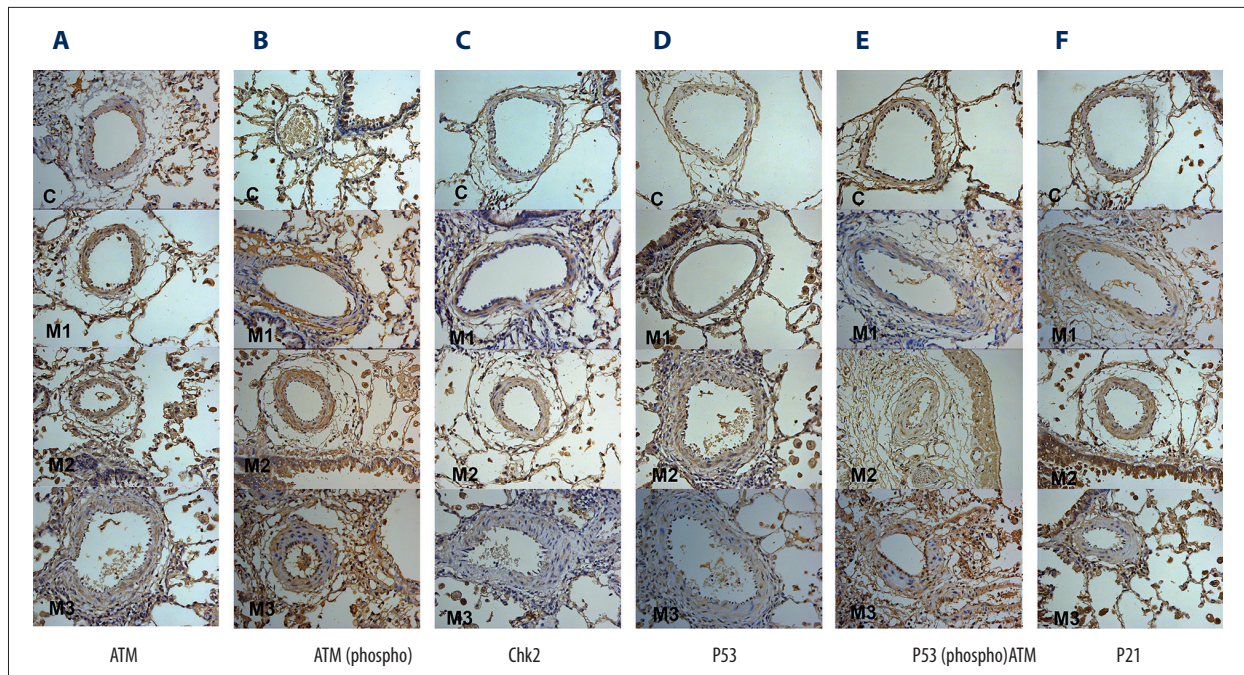
Figure 2. Representative images of immunohistochemistry experiments (×400). From left to right: (**A**) Increased ATM expression in Group M1 compared with Group C, and decreased ATM expression in Group M3 compared with Group M1 and M2. (**B**) Increased phosphorylated ATM expression in Group M1 and M2 compared with Group C, and decreased phosphorylated ATM expression in Group M3 compared with Group M1 and M2. (**C**) Increased Chk2 expression in Group M1 and M2 compared with Group C, and decreased Chk2 expression in Group M3 compared with Group M1 and M2. (**D**) Increased P53 expression in Group M1 compared with Group C, and decreased P53 expression in Group M2 and Group M3 compared with Group M1. (**E**) Increased phosphorylated P53 expression in Group M1 compared with Group C, and decreased phosphorylated P53 expression in Group M2 and Group M3 compared with Group M1. (**F**) Increased P21 expression in Group M1 and M2 compared with Group C, and decreased P21 expression in Group M3 compared with Group M1 and M2.

in 96-well plates with $5×10^4$ cells/well. Different concentrations of KU60019 were added to the cells: 0.1 µM, 0.3 µM, 0.5 µM, and solvent for 24 h. MTT tetrazolium (Sigma-Aldrich, St. Louis, USA) was added to the cells for 4 h. After that, the formation of colored formazan was assessed by a spectrophotometer at 570 nm. The procedure was performed 3 times for each sample.

Apoptosis of PA-SMACs

Apoptosis was evaluated by TUNEL. The PA-SMCs were divided into 4 groups: Solvent Group: cells without treatment, KU60019 Group: cells treated with 1 µM KU60019 for 24 h, H_2O_2 Group: cells treated with 200 µM H_2O_2 for 24 h,

KU60019 + H_2O_2 Group: cells treated with 1 µM KU60019 and 200 µM H_2O_2 for 24 h.

The TUNEL reaction mixture (Roche, Switzerland) was added to the cells according to the manufacturer's instructions. Then, apoptosis was detected with a fluorescence microscope. Quantification of apoptosis was performed in 5 images for each sample.

Statistics

Statistical analyses were performed by SPSS 23.0. Scaler variables were tested for normal distribution, and data following normal distribution were expressed as mean ±SE. The results were analyzed by ANOVA. $P<0.05$ was considered to indicate a statistically significant difference.

Results

Animal model

The animal models were successfully established and showed signs of severe PAH. The PAP in Group M1 was higher than in the Control Group, and it became much higher in Groups M2 and M3, where severe PAH formed. The pressure in Group M2 and Group M3 showed no significant differences (Figure 1A). The RV/(LV+S) also kept significantly increasing in Group M1 and Group M2 when compared with the Control Group; however, there are no significant differences between Group M2 and Group M3 (Figure 1B). HE staining of right lungs in the Control Group seemed normal, but showed thickened vascular muscle

cells in Group M1. HE staining of right lungs demonstrated obvious vascular lesions in Group M2 and Group M3, which suggested the formation of severe PAH (Figure 1C).

Immunohistochemistry

To examine the expression of the ATM-Chk2 pathway on vascular smooth muscle cells, immunohistochemistry was performed. Results show that the expression of ATM, Chk2, and P21 increased in Groups M1 and M2 compared with the Control Group, and decreased in Group M3 when compared with Groups M1 and M2. Furthermore, expression of P53 increased in Group M1 compared with the Control Group, and decreased in Groups M2 and M3 compared with Group M1 (Figure 2). This analysis suggested that expression of the ATM-Chk2 pathway in vascular smooth muscle cells increased in the early stages of PAH, but decreased in the late stages once severe PAH was formed.

RT-PCR

To determine the expression of genes involved in the ATM-Chk2 pathway in the lung, RT-PCR was performed. Results demonstrated that in Groups M1 and M2, the expression of ATM, Chk2, P53, and P21 increased compared with the Control Group, whereas
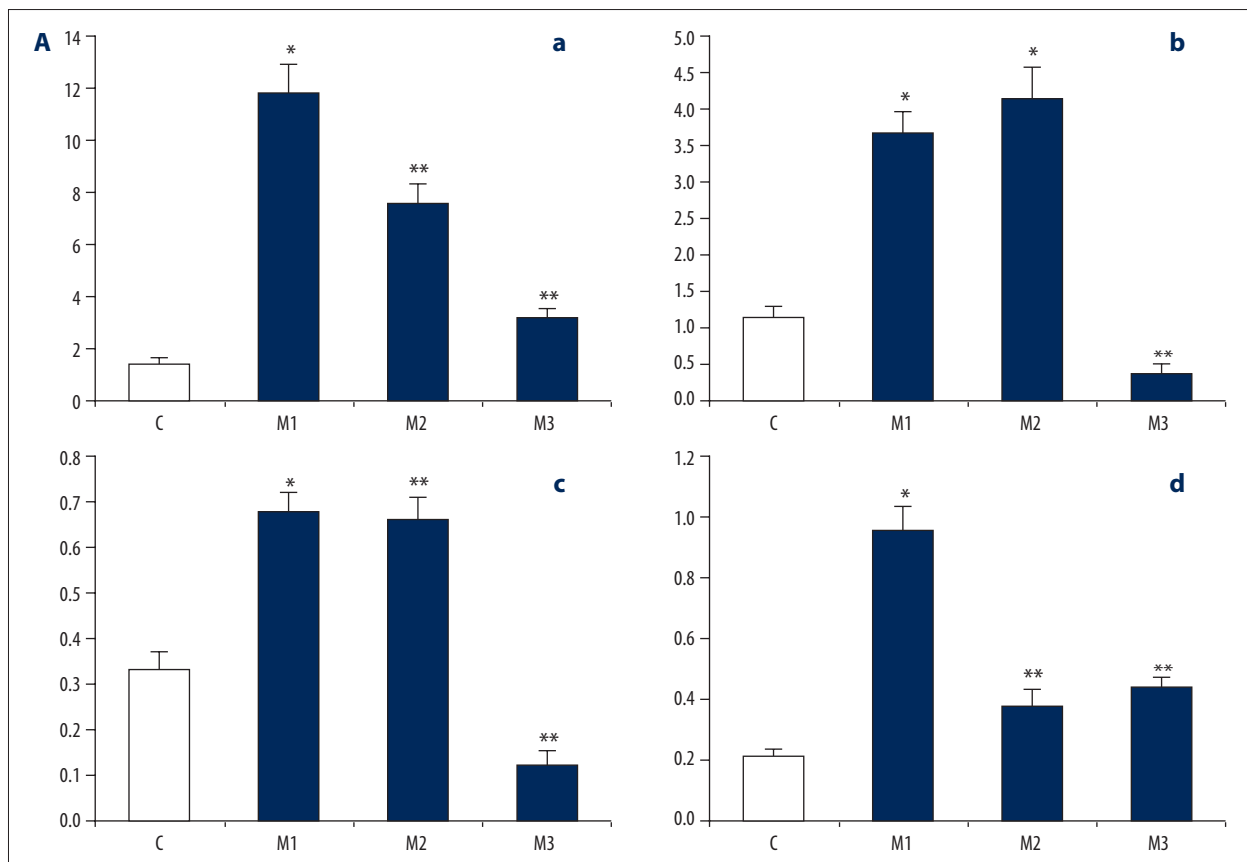
it decreased in Group M3 compared with Group M1 (Figure 3A). This result suggests that expression of the ATM-Chk2 pathway in the lung increased in early stages of PAH (Group M1), but decreased in late stages of PAH (Group M2 or M3).

Western blotting

To determine the expression of proteins involved in the ATM-Chk2 pathway in the lung, Western blotting was performed. Results show that the expression of ATM, Chk2, P53, and P21 gradually increased in Group M1 and Group M2 compared with the Control Group. Proteins reached the highest expression in Group M2. According to the stereology study, severe PAH formed in Group M2; however, in Group M3, where severe PAH still existed, protein expression significantly dropped compared with that in Group M1 and Group M2 ($P < 0.05$) (Figure 3B). The results suggest that the expression of proteins from the ATM-Chk2 pathway in the lung increased in early stages of PAH (Group M1), but decreased in late stages (Group M3). These results are consistent with the results obtained with RT-PCR.

Effect of KU60019 on the proliferation of PA-SMCs

MTT was performed to test the effect of KU60019 on the cell growth of PA-SMCs. We tested the effect of KU60019 with
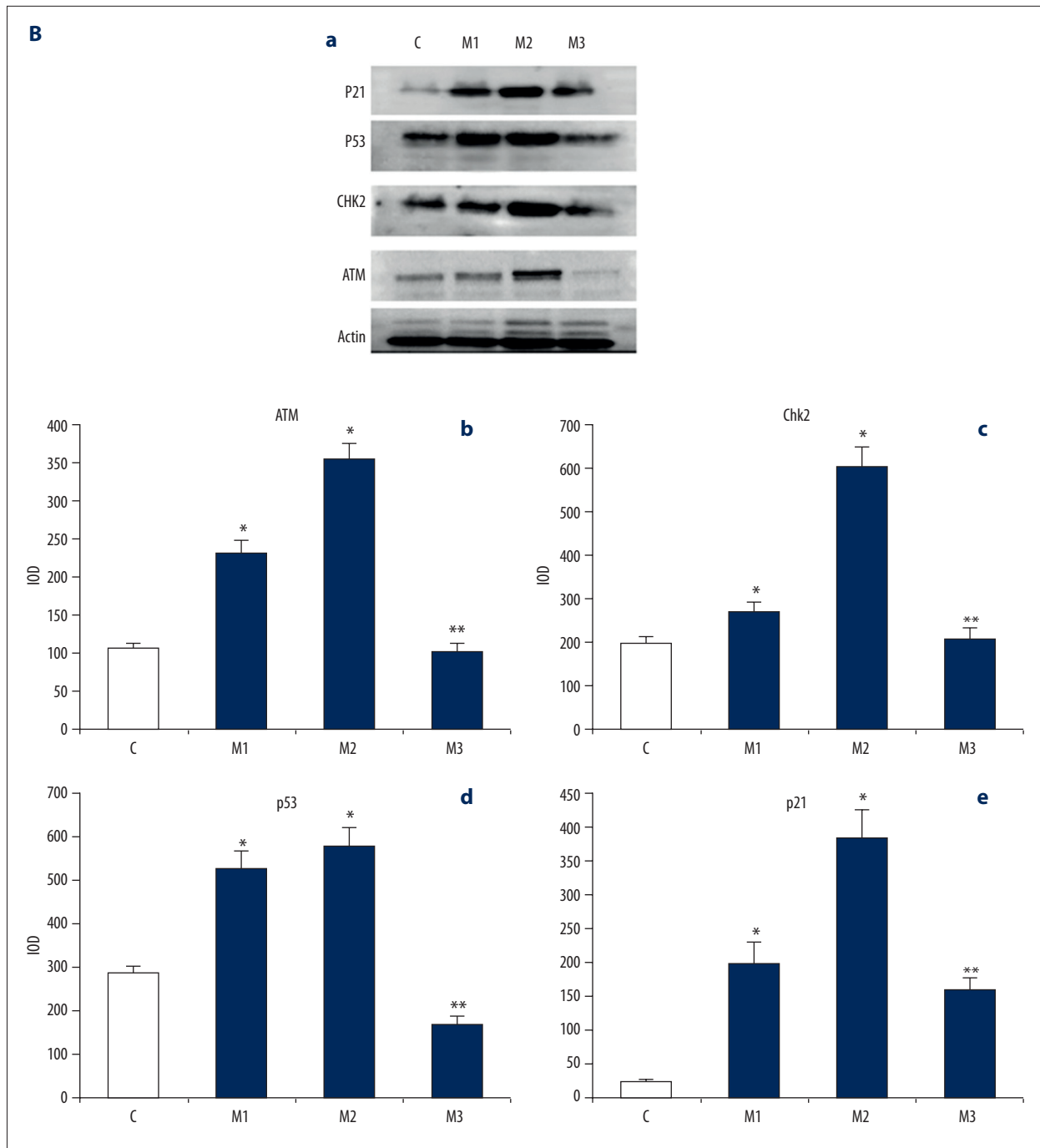
Figure 3. (**A**) RT-PCR of ATM and its downstream genes. (**a**) * Expression of ATM increased in Group M1 compared with Group C (p<0.001); ** expression of ATM decreased in Group M2 and M3 compared with Group M1 (p=0.002 and p<0.001, respectively). (**b**) * Expression of Chk2 increased in Group M1 and M2 compared with Group C (p<0.001); ** expression of Chk2 decreased in Group M3 compared with M1 and M2 (p<0.001). (**c**)* Expression of P53 increased in Groups M1 and M2 compared with Group C (p=0.01 and p=0.02, respectively); ** expression of P53 decreased in Group M3 compared with M1 and M2 (p<0.001). (**d**) * Expression of P21 increased in Group M1 compared with Group C (p<0.001); ** expression of P21 decreased in Group M2 and M3 compared with M1 (p<0.001 and p<0.001, respectively). Although there was an apparent increase in Group M3 when compared with Group M2, there were no statistically significant differences (p=0.5). (**B**) Western blotting on rat lungs. (**a**) Protein levels of ATM, Chk2, P53, and P21 in rat lungs. (**b–e**) Assessment of ATM, Chk2, P53, and P21 levels by IOD. * p<0.05 *vs*. Group C, ** p<0.05 *vs*. Group M2.
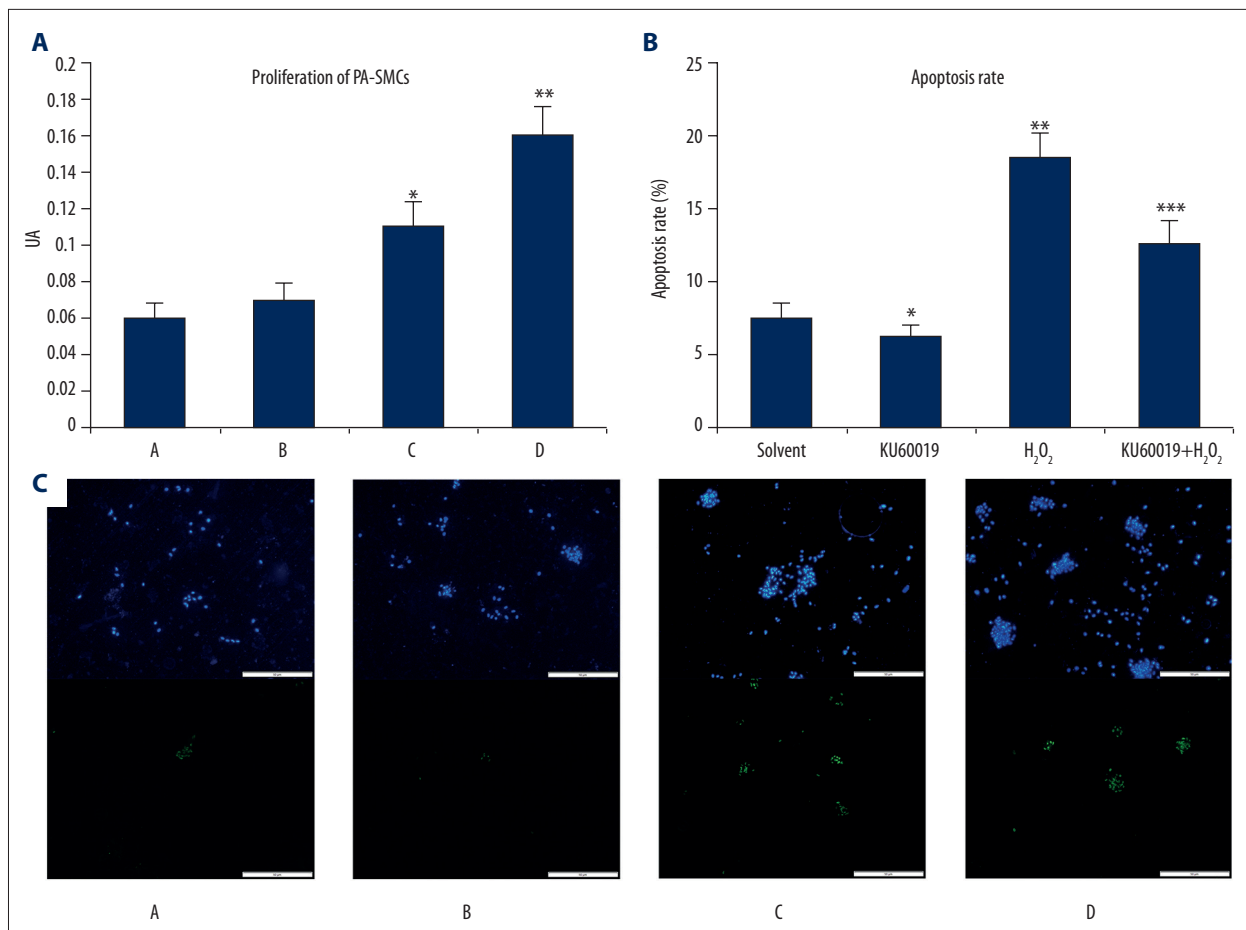
Figure 4. (**A**) Proliferation of PA-SMCs after treatment with different concentrations of KU60019. With increasing concentrations of KU60019, PA-SMCs showed increased activity in the 0.3 μM and 0.5 μM groups. With a concentration of 0.5 μM, the increase in cell growth was more noticeable, when compared to other groups. (A) solvent group, (B) 0.1 μM KU60019, (C) 0.3 μM KU60019, (D) 0.5 μM KU60019. * p<0.001 compared with base group, ** p<0.001 compared with base group, p=0.012 compared with 0.3 μM group. (**B**) Apoptosis rate of PA-SMCs with different treatments. * p=0.096 compared with solvent group, ** p<0.001 compared with solvent group, *** p=0.008 compared with H_2O_2 group. (**C**) Representative images of TUNEL assay with DAPI. Cell nuclei are blue (DAPI), apoptotic cells are green. (A) solvent group, (B) KU60019 group, (C) H_2O_2 group, (D) KU60019 + H_2O_2 group.

different concentrations, including 0.1 μM, 0.3 μM, and 0.5 μM. The results demonstrated that at a concentration of 0.5 μM, KU60019 increased cell growth more noticeably compared with other groups (Figure 4A).

Effect of KU60019 on the apoptosis of PA-SMCs

The TUNEL assay demonstrated the anti-apoptosis effect of 0.5 μM KU60019 on PA-VMCs (Figure 4B, 4c). We evaluated different concentrations of H_2O_2 and chose 200 μM H_2O_2, which induced maximum apoptosis. KU60019 clearly reduced the apoptosis rate in the presence of H_2O_2 and seemed to reduce apoptosis when compared with the solvent group without H_2O_2 (p=0.096). This result suggests that by reducing the expression of ATM, cell apoptosis could also be reduced.

Discussion

ATM is considered a core factor in DDR. When DNA damage occurs, the ATM pathway, including ATM and its downstream genes, is activated to finalize the DNA repair [18,19]. In case of double-strand breaks in DNA, the ATM pathway is activated via phosphorylation of ATM. The phosphorylated ATM combines with damaged DNA and phosphorylates the Chk2 protein. This activates P53, followed by the activation of other downstream proteins to form the cascade effect for the repair of double-strand breaks. Cells and organs survive with malfunction or mutations in the ATM at the cost of genome instability or development of cancer [18]. Research on the function of the ATM-Chk2 pathway is mainly based on mutation analyses of the pathway genes in tumors. These studies, which

supported the existence of DDR in PAH patients [15,16], provided us with the idea that the ATM pathway participates in DNA repair of PAH patients.

Several studies provided evidence supporting a similarity in abnormal proliferation between PA-SMCs in severe PAH and tumors. In severe PAH, there is a decrease in the expression of type II bone morphogenetic protein receptor (BMPR II) in PA-SMCs [20]. This research revealed the insensitivity of PA-SMCs to growth inhibitory signals, similar to tumors, as BMPR II can inhibit cell proliferation. Similar to tumor cells, the metabolism of mitochondria and the oxidation-reduction signal pathway were abnormal in PA-SMCs of severe PAH, which resulted in depolarization of the cell membrane, increased calcium and potassium in the cytoplasm, and increased ability to resist apoptosis [21,22]. Recent studies suggested that mircroRNA-17 participates in both PA-SMCs proliferation and cervical cancer tumorigenesis [23,24]. Based on the similarity between PA-SMCs of severe PAH and tumors, and on the existence of DDR in the 2 types of diseases, we considered that the ATM pathway plays an important role in the formation of PAH, just as in tumors.

In our study, immunohistochemistry, RT-PCR, and Western blot results demonstrated that in the formation of PAH (Group M1), the expression of downstream effectors of the ATM pathway (ATM, Chk2, P53, and P21) increased significantly. As the disease progressed to severe PAH (Group M3), the expression of ATM, Chk2, P53, and P21 decreased significantly. The results suggest that the ATM pathway was activated in early and middle stages of PAH. However, in later stages of PAH, expression of the ATM pathway significantly decreases. This phenomenon

indicates that the ATM-Chk2 pathway plays a key role in early stages of PAH, but not in later stages.

To further verify the role of the ATM pathway in the proliferation and apoptosis of PA-SMCs, we used KU60019 to inhibit the expression of ATM in primary cultured cells. We used cells in the middle stages of PAH, where ATM is upregulated. Results show that inhibition of ATM was followed by increased proliferation and reduced apoptosis of PA-SMCs. In other words, in the middle stages of PAH, the upregulated ATM seems to prevent PA-SMCs from growth in order to slow down the development of PAH. It is well established that ATM signaling arrests proliferation and induces apoptosis [25–27]. In our study, inhibition of ATM signaling seemed to enhance PA-SMCs proliferation. A previous study suggested that inhibition of P53 resulted in increased PA-SMCs proliferation [28], and KU60019 markedly reduced the level of P53 [29]. These findings suggest that KU60019 induces cell proliferation through inhibition of P53.

Conclusions

In summary, this study revealed the expression of the ATM pathway in a rat PAH model. Additionally, we demonstrated the modulating role of the ATM pathway in the proliferation and apoptosis of rat PA-SMCs. In this study, expression of the ATM pathway increased in early stages of PAH formation, but decreased in late stages when severe PAH developed. In primary cultured PA-SMCs from middle stages of PAH, the ATM inhibitor KU60019 increased cell proliferation and inhibited cell apoptosis.

References:

1. Morrell NW, Adnot S, Archer SL et al: Cellular and molecular basis of pulmonary arterial hypertension. J Am Coll Cardiol, 2011; 54: S20–31

2. Yi ES, Kim H, Ahn H et al: Distribution of obstructive intimal lesions and their cellular phenotypes in chronic pulmonary hypertension. A morphometric and immunohistochemical study. Am J Respir Crit Care Med, 2000; 162: 1577–86

3. Rosenblum WD: Pulmonary arterial hypertension: Pathobiology, diagnosis, treatment, and emerging therapies. Cardiol Rev, 2010; 18(2): 58–63

4. Jonigk D, Golpon H, Bockmeyer CL et al: Plexiform lesions in pulmonary arterial hypertension composition, architecture, and microenvironment. Am J Pathol, 2011; 179: 167–79

5. Li D, Zhang C, Song G et al: VEGF regulates FGF-2 and TGF-betM1 expression in injury endothelial cells and mediates smooth muscle cells proliferation and migration. Microvasc Res, 2009; 77: 134–42

6. Sakao S, Taraseviciene-Stewart L, Wood K et al: Apoptosis of pulmonary microvascular endothelial cells stimulates vascular smooth muscle cell growth. Am J Physiol Lung Cell Mol Physiol, 2006; 291: L362–68

7. Rai PR, Cool CD, King JA et al: The cancer paradigm of severe pulmonary arterial hypertension. Am J Respir Crit Care Med, 2008; 178(6): 558–64

8. Sakao S, Tatsumi K: Vascular remodeling in pulmonary arterial hypertension: Multiple cancer-like pathways and possible treatment modalities. Int J Cardiol, 2011; 147(1): 4–12

9. Aguilera A, Gomez-Gonzalez B: Genome instability: A mechanistic view of its causes and consequences. Nat Rev Genet, 2008; 9(3): 204–17

10. Lukas J, Lukas C, Bartek J: More than just a focus: The chromatin response to DNA damage and its role in genome integrity maintenance. Nat Cell Biol, 2011; 13(10): 1161–69

11. Bhatti S, Kozlov S, Farooqi AA et al: ATM protein kinase: The linchpin of cellular defenses to stress. Cell Mol Life Sci, 2011; 68(18): 2977–3006

12. Kastan MB, Lim DS: The many substrates and functions of ATM. Nat Rev Mol Cell Biol, 2000; 1: 179–86

13. Ide H, Lu Y, Yu J et al: Testosterone promotes DNA damage response under oxidative stress in prostate cancer cell lines. Prostate, 2012; 72: 1407–11

14. Greiner TC, Dasgupta C, Ho VV et al: Mutation and genomic deletion status of ataxia telangiectasia mutated (ATM) and P53 confer specific gene expression profiles in mantle cell lymphoma. Proc Natl Acad Sci USA, 2006; 103: 2352–57

15. Aldred MA, Comhair SA, Varella-Garcia M et al: Somatic chromosome abnormalities in the lungs of patients with pulmonary arterial hypertension. Am J Respir Crit Care Med, 2010; 182: 1153–60

16. Majka SM, Skokan M, Wheeler L et al: Evidence for cell fusion is absent in vascular lesions associated with pulmonary arterial hypertension. Am J Physiol Lung Cell Mol Physiol, 2008; 295(6): L1028–39

17. Yin Y, Wu X, Yang Z et al: The potential efficacy of R8-modified paclitaxel-loaded liposomes on pulmonary arterial hypertension. Pharm Res, 2013; 30: 2050–62

18. Smith J, Tho LM, Xu N, Gillespie DA: The ATM-Chk2 and ATR-Chk1 pathways in DNA damage signaling and cancer. Adv Cancer Res, 2010; 108: 73–112

This work is licensed under Creative Common Attribution-NonCommercial-NoDerivatives 4.0 International (CC BY-NC-ND 4.0)

4399

Indexed in: [Current Contents/Clinical Medicine] [SCI Expanded] [ISI Alerting System] [ISI Journals Master List] [Index Medicus/MEDLINE] [EMBASE/Excerpta Medica] [Chemical Abstracts/CAS] [Index Copernicus]

19. Matsuoka S, Ballif BA, Smogorzewska A et al: ATM and ATR substrate analysis reveals extensive protein networks responsive to DNA damage. Science, 2007; 216: 1160–66

20. Aldred MA, Comhair SA, Varella-Garcia M et al: Somatic chromosome abnormalities in the lungs of patients with pulmonary arterial hypertension. Am J Respir Crit Care Med, 2010; 182: 1153–60

21. Morrell NW: Pulmonary hypertension due to BMPR2 mutation: A new paradigm for tissue remodeling? Proc Am Thorac Soc, 2006; 3(8): 680–86

22. Archer SL, Gomberg-Maitland M, Maitland ML et al: Mitochondrial metabolism, redox signaling, and fusion: A mitochondria-ROS-HIF-1alpha-Kv1.5 O2-sensing pathway at the intersection of pulmonary hypertension and cancer. Am J.Physiol Heart Circ Physiol, 2008; 294(2): H570–78

23. Lu Z, Li S, Zhao S, Fa X: Upregulated mirR-17 Regulates hypoxia-mediated human pulmonary artery smooth muscle cell proliferation and apoptosis by targeting mitofusin 2. Med Sci Monit, 2016; 22: 3301–8

24. Ji F, Wuerkenbieke D, He Y, Ding Y: Long noncoding RNA hotair: An oncogene in human cervical cancer interacting with microRNA-17-5p. Oncol Res, 2017 [Epub ahead of print]

25. Zeng YC, Xing R, Zeng J et al: Sodium glycididazole enhances the radiosensitivity of laryngeal cancer cells through downregulation of ATM signaling pathway, Tumour Biol, 2016; 37: 5869–78

26. Neumann J, Yang Y, Köhler R et al: Mangrove dolabrane-type of diterpenes tagalsins suppresses tumor growth via ROS-mediated apoptosis and ATM/ATR-Chk1/Chk2-regulated cell cycle arrest. Int J Cancer, 2015; 137: 2739–48

27. Chou WC, Hu LY, Hsiung CN, Shen CY: Initiation of the ATM-Chk2 DNA damage response through the base excision repair pathway. Carcinogenesis, 2015; 36: 832–40

28. Jacquin S, Rincheval V, Mignotte B et al: Inactivation of P53 is sufficient to induce development of pulmonary hypertension in rats. PLoS One, 2015; 10(6): e0131940

29. Zhu Y, Mao C, Wu J et al: Improved ataxia telangiectasia mutated kinase inhibitor KU60019 provides a promising treatment strategy for non-invasive breast cancer. Onco Lett, 2014; 8(5): 2043–48